NPC Natural Product Communications

2012
Vol. 6
No. 0
1 - 3

Catalytic and Molecular Properties of Rabbit Liver Carboxylesterase Acting on 1,8-Cineole Derivatives

María del H. Loandos[a], Ana C. Muro[a], Margarita B. Villecco[a], Marcelo F. Masman[b,c], Paul G.M. Luiten[b], Sebastian A. Andujar[c,d], Fernando D. Suvire[c] and Ricardo D. Enriz[c,d]*

[a]*Instituto de Química Orgánica, Facultad de Bioquímica Química y Farmacia, Universidad Nacional de Tucumán, Ayacucho 471, S. M. de Tucumán, T4000INI. Argentina*

[b]*Department of Molecular Neurobiology, University of Groningen, Nijenborgh 7,9747 AG Groningen, The Netherlands*

[c]*Departamento de Química, Universidad Nacional de San Luis, Chacabuco 917, San Luis 5700. Argentina.*

[d]*IMIBIO-SL. Instituto Multidisciplinario de Investigaciones Biológicas, San Luis CONICET*

denriz@unsl.edu.ar

Received: April 12th, 2012; Accepted: XX, 2012

Rabbit liver carboxylesterase (rCE) was evaluated as the catalyst for the enantioselective hydrolysis of (±)-3-endo-acetyloxy-1,8-cineole [(±)-**4**], which yields (1S,3S,4R)-(+)-3-acetyloxy-1,8-cineole [(+)-**4**] and (1R,3R,4S)-(-)-3-hydroxy-1,8-cineole [(-)-**3**]. Enantioselective asymmetrization of meso-3,5-diacetoxy-1,8-cineol (**5**) gives (1S,3S,4R,5R)-(-)-3-acetyloxy-5-hydroxy-1,8-cineole (**6**), with high enantioselectivity. rCE has been chosen to perform both experiments and molecular modeling simulations. Docking simulations combined with molecular dynamics calculations were used to study rCE-catalyzed enantioselective hydrolysis of cineol derivatives. Both compounds were found to bind with their acetyl groups stabilized by hydrogen bond interactions between their oxygen atoms and Ser221.

Keywords: 1,8-Cineole, Rabbit liver carboxylesterase, Molecular Modeling, Docking.

Previously we reported seven new homochiral compounds derived from cineole by enantioselective hydrolysis and asymmetrization using porcine liver esterase (PLE) with high enantioselectivity [1]. Considering that the molecular structure of rabbit liver carboxylesterase (rCE) is available from the Protein Data Bank (PDB code: 1K4I) [2], with a rather acceptable degree of accuracy (2.5 Å), we have chosen this enzyme to carry out both experiments and molecular modeling simulations. Thus, in the present report we extended our previous studies using rCE. Here we report some catalytic properties and characteristics using (±)-3-endo-acetyloxy-1,8-cineole [(±)-**4**] and (±)-3,5-cis,cis-diacetyloxy-1,8-cineole [(±)-**5**] as substrates. Furthermore, we investigated the optimal reaction conditions in terms of temperature, pH, and inorganic salt content. It is known that the promiscuous mammalian carboxylesterases (CEs) act on a wide variety of ester, amide and thioester substrates [3] and are able to metabolize numerous analgesic and narcotic compounds [4-11]. Esterases share a common structural framework, active site and two-step serine hydrolase mechanism [12,13]. The active site contains a serine hydrolase catalytic triad, which is composed of a Ser, a His and either Asp or a Glu residue. A rabbit liver CE (rCE) was found to be one of the most efficient enzymes identified to date in the activation of the anticancer prodrug CPT-11(Irinotecan, 7-ethyl-10-[4-(1-piperidino)-1-piperdidino] carbonyloxycamptothecin) [8]. However, human liver carboxylesterase CE-1 (hCE1), the human homolog of rCE (81% sequence identity), is unable to process CPT-11 [14,15]. It has been proposed that the differences these enzymes show in activity toward substrates are based on the way they orient molecules into their active sites [16,17].

Recently, computer-based modeling methodology has been increasingly used to understand the mechanism and selectivity of enzyme-catalyzed reactions and suggest how to change the selectivity of these reactions by modification of either the enzyme or the substrate structures [18,19]. To our knowledge, there is no published record on the application of computer-based modeling to describe the molecular interactions involved in cineols recognition by esterases.

The second part of this study focuses on the development of a computational approach able to successfully predict and rationalize the enantioselective hydrolysis of cineol derivatives by the rCE enzyme.

Enantioselective hydrolysis of cineol derivatives: rCE was effective for separation of enantiomers of (±)-**4** and also asymmetrization of meso-diacetate **5**. The enantioselective hydrolysis of (±)-**4**, after incubation for 12 d, showed a mixture of (-)-**3**, unaffected (+)-**4** (90.8 % ee) and (-)-**4**, which were readily separated by column chromatography on Si gel. The employed chiral GC column was ineffective to resolve the enantiomers of alcohol rac-**3**. On the other hand the asymmetrization of meso-diacetate **5**, after incubation for 4 d, provides the enantiomerically pure monoester (-)-**6**.

To compare enantioselective hydrolysis with PLE and rCE we employed reaction media with pH 7. In contrast to the previous results obtained with PLE, the hydrolysis of (±)-**4** with rCE showed no enantioselectivity, catalysing its complete hydrolysis giving the racemic alcohol **3**. It is known that the optimum pH of carboxylesterases lies in the slightly alkaline range between 7.5 and

9 [20]. Good yields and high enantioselectivity for hydrolysis of (±)-**4** and meso-**5** were obtained at pH 8.5 with 70 mM Tris-HCl, and 0.3% Triton X-100 solution as reaction medium. It is interesting to note that this pH-dependent enantioselectivity has already been reported for other carboxylesterases. In particular James *et al.* [21] reported on the effect of pH on the *Candida rugosa* lipase enantioselective hydrolysis of ibuprofen esters. In this study we observed that group-R is hydrolyzed faster than group-S. This is in full agreement with regioselective deacylations performed with PLE, previously described [22].

The absolute configuration of chiral compounds was determined to be R by chemical conversion to the known compounds and by comparison of the specific rotations with previous reports and comparison with pure compounds [1].

Molecular modeling: The molecular modeling study was performed in two steps: i) docking analyses of compounds **4S, 4R** and **5** (Figure 1) and ii) molecular dynamic (MD) simulations performed for some complexes in order to verify their stabilities and the influence of the molecular interactions at the active site.

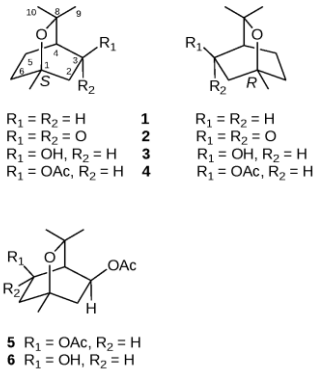

Figure 1: Chemical structures of cineole derivatives **1-6**

When the rCE structure reported by Bencharit *et al.* (PDB codes: 1K4Y) and the rCE structure obtained here from homology are superimposed, a high degree of similarity can be identified (94 %). The superimposed structures can be appreciated in Figure 2. The enzyme is composed of a catalytic domain, an alpha beta domain and a regulatory domain, which have been previously described in detail by Bencharit *et al*. [2]. Ser 221, Glu 353 and His 467, conserved residues in the human CEs, form the rCE catalytic triad (Figure 3). This Figure displays the main residues lining the rCE cavity. It should be noted that such a site is surrounded by hydrophobic residues with a significant abundance of alkyl side-chains.

Docking results: We attempted to predict the structures of the intermolecular complexes formed between compounds **4** and **5** with rCE. However, it should be noted that compound **4** possesses two different configurational isomers (**4R** and **4S**) (Figure 4) and, therefore, both isomeric forms were taken into account in this analysis.

In this step, with the aim to determine whether optimized complexes corresponded to productive binding modes, they were analyzed by combining two criteria used in previous studies dealing with molecular modeling of carboxylesterases. The first criterion is the rmsd between the enzyme structure in the complex and its initial crystal structure. Even though some enzymes may undergo relatively large conformational changes upon the binding substrates, characterized by rmsd values up to 6 Å [23], we chose here a lower rmsd value (2.5 Å rms deviation over Ser221 Cα positions). The second criterion is that the complexes must display interaction between the ligand and Ser221. We assumed that, in order to be considered as reactive, the acetate group must be placed at 4 Å

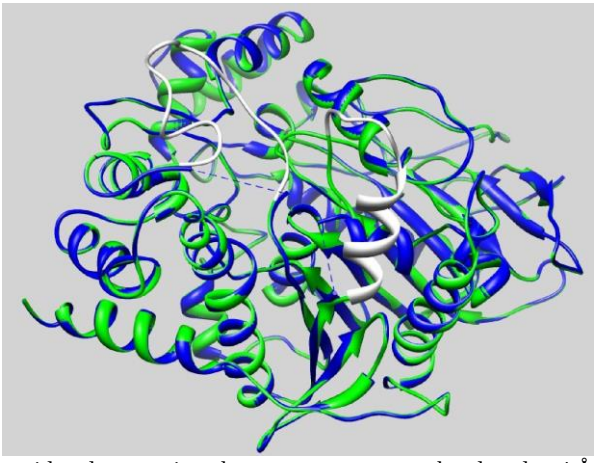

Figure 2: Spatial view of the rCE enzyme. In blue, structure obtained from the PDB (code 1K4Y), in green, that obtained from homoly study reported here, in which residues 355-370 (loop 1) and 450-466 (loop 2) are shown in white.

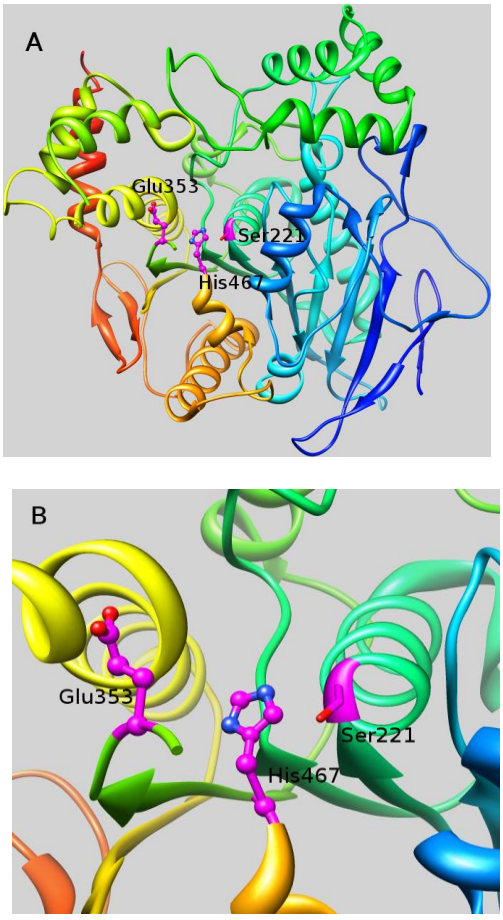

Figure 3: a) Spatial view of the rCE enzyme obtained from MD simulations using the chimera program as graphic interface. In this figure the binding pocket is denoted with a square. b) Spatial view of the binding pocket denoting the most relevant aminoacids (Ser221, Glu353 and His467).

maximum from the OH of Ser221. Thus, the 50 independent docking conformations for each ligand (**4R**, **4S** and **5**) were clustered according to the above criteria.

In the case of **4R** the 50 complexes presented the ligand in two orientations: the OI of the acetyl group orientated towards Ser221, and the OIII interacting with the Ser221, with the former being the the preferred form. The same results were also obtained for the OIV

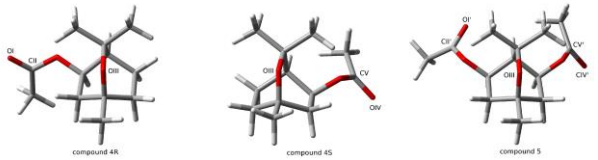

Figure 4: Structural profiles of the compounds evaluated using molecular modeling techniques (compounds **4R**, **4S** and **5**). It should be noted that compound **4S** is the specular image of **4R** and, therefore, its enantiomer. The spatial arrangements of OI, CII, (**4R**), OIV, CV (**4S**), OI`, CII`, OIV`, CV` (**5**) and OIII are shown here.

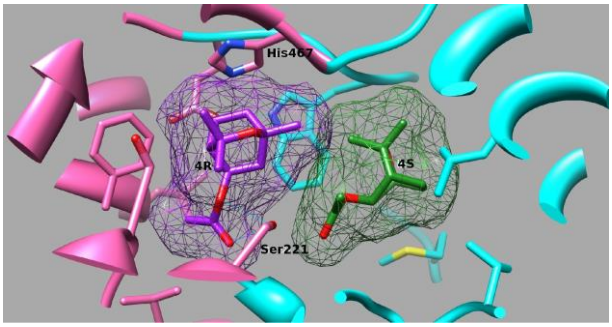

Figure 5: Interactions of isomers **4R** (fuchsia) and **4R** (green) at the Binding pocket of rCE. This spatial view was obtained from the overimposition of respective output files of MD simulations obtained for both isomers. The stabilizing interactions between these compounds with Ser221 and His467 are shown in this figure.

of the **4S** isomer. Comparing the complexes obtained for **4R** and **4S**, the docking results predict that the complexes of isomer **4R** are the preferred ones, which is in agreement with our experimental results. In the productive complexes, the reactive groups of both isomers are located at the cavity, but with distinct orientations, one perpendicular to the other (Figure 5). In order to explain such behavior, we simulated the docking of these isomers employing another approach. Thus, we complemented our study by molecular dynamics simulations on the productive complexes (2ns at 298 K) to verify the stability of the interactions and to evaluate the dynamic behavior of the docked ligands. We aimed to refine the models, accounting for the flexibility of both enzyme and ligand, and to check the complex temporal stability (results shown in the following section).

Among the complexes obtained for compound **5**, three possible orientations were found: The OI`, the OIII and OIV` orientated towards Ser221. For these complexes, the preferred form is when Ser221 interacts with the oxygen atom OI`. These results are also in complete agreement with our experimental data.

The considerations described above find supportive evidence when analyzing the putative enzyme-ligand complexes. Thus, the ligand accommodates the acetyl group with the carbon atom of the carbonyl group reasonably close to Ser 221 (Figure 5). Furthermore, the rest of the molecule generates apolar interactions with aromatic residues thus reinforcing the stability of the complex.

MD simulations: It must be pointed out that the serine hydrolase catalytic mechanism is well known and there are, in the literature, many reports about this interesting problem. Thus, our aim in this theoretical study is not focused on performing another study about the molecular mechanism of action for this enzyme. In fact our objective is less ambitious; we wish to obtain from the MD simulations a reasonable explanation for the obtained experimental results.

Molecular dynamics simulations were carried out on rCE complexed with **4R, 4S** and **5**, our objective being to investigate the stability of the computed complexes and the influence of intermolecular interactions on the *in situ* behavior of ligands. Thus, twelve MD runs were carried out to simulate rCE complexed with ligands **4R**, **4S** and **5**, six independent MD runs for **4R** and **4S** (three for each isomer), and six independent runs for compound **5** (three for each acetyl group) (see Figure 4). In order to evaluate the stability of these complexes, their transacetyl distances were monitored along the trajectory. Thus, the resulting trajectories were analyzed by monitoring how the distance between Ser 221 and the target acetyl group in ligands varied during the simulations (2ns). Comparing the results obtained for isomers **4R** and **4S**, there is a significant difference between the two MD simulations since the acetyl group in **4R** remained markedly closer to Ser221 than for **4S** (0.4 nm vs 0.7 nm, Figure 6). Interestingly, only the acetyl group of compound **4R** reached distances inferior to 0.4 nm from Ser221. Furthermore, maximal fluctuations in these distances were weak (about 0.35-0.45 nm). These results obtained from MD simulations reinforce our experimental results about regioselectivity in rCE catalyzed acylation of cineol derivatives.

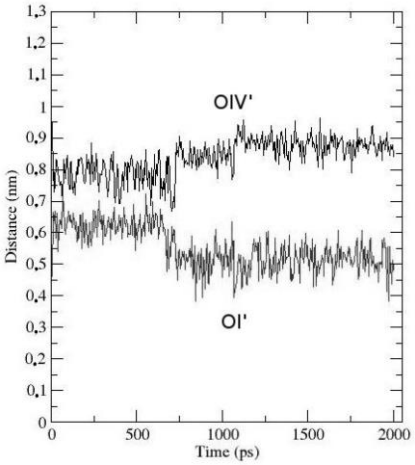

Figure 6: Evolution of the distance between acetyl group of isomers **4R** and **4S** with Ser221 with time during the simulation

Regarding MD simulations involving compound **5**, we monitored the distance between its two acetyl groups and Ser 221. MD simulation results were mainly analyzed for OI` and OIV` because it has been previously reported that the acetyl group is interacting with Ser 221 and either the OI` or OIV` [18]. Here, a totally different result was obtained depending on which of the acetyl groups is interacting. Indeed, the OI` remained anchored to the catalytic site displaying distances of about 0.45 nm, whereas OIV` showed larger distances of about 0.9 nm. This differential behavior can be appreciated in Figure 7. Once again these results are in agreement with our experimental results indicating that the hydrolysis can take place only on the acetyl group possessing OIV` in compound **5**.

The above considerations of the rCE cavity shed light on some key features common to all complexes examined. First, the acetyl group in the compounds must come close to the hydroxyl function of Ser221. This mandatory contact was used to select the best binding modes for each ligand. In addition, the soundness of docking results was also verified by checking the distance between the oxygen atom of the cineols and the OH group of Ser 221.

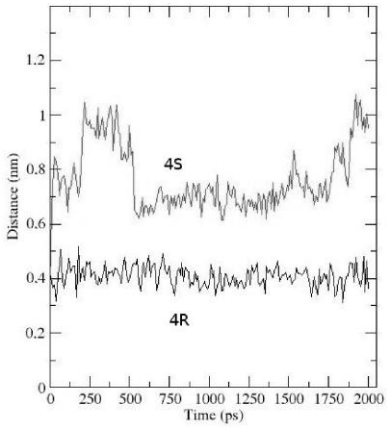

Figure 7: Evolution of the distance between both acetyl groups of compound **5** with Ser221 with time during the simulation.

Although the rCE efficiency as a catalyst for enantioselective hydrolysis of cineole derivatives is very low when compared with pig liver esterase (PLE) [24], our results allow us to have a good idea of the molecular interactions involved in such a process.

Conclusions: Enantioselective hydrolysis of a meso form of cineolyl acetate (**4**) was effective using rCE, as well as enantioselective assymetrization of meso-diacetate **5**, in both with high enantiomeric excess. The enzyme-mediated reaction was found to be selective for the (*R*)-ester; this is in accordance with the result previously obtained by our group with porcine liver esterase (PLE) [1]. Clearly, rCE is a potential alternative for enantioselective biotransformations against the more widely used pig liver esterase.

In order to understand the orientations of compounds **4R**, **4S** and **5** within the rCE binding pocket, the observed interactions between these ligands and the enzyme residues were compared. Thus, the presence of the essential interactions between the acetate carbonyl oxygen (Ace:O) and Ser221 were monitored. The visual analysis of trajectories shows that the distance OI`—OH is smaller for isomer **4R** (about 3.0 Å) than for OIV`—OH of **4S** (about 6.0) indicating that **4R** is more bent in rCE compared with **4S**. The MD simulations are able to explain the selective behavior of rCE on the acetyl groups of compound **5** as well. Thus, our molecular modeling study provides a molecular-level explanation for the experimentally observed regioselectivity of rCE towards the acetyl groups of cineol derivatives **4** and **5**. A combined docking and molecular dynamics approach was used to study the positions, the orientations, the interactions of these two compounds in the active site of rCE, and the accessibility of their acetyl groups to the catalytic residues. All these factors are important to determine if a given ligand binding mode is productive or not, thus allowing the elucidation of the regioselectivity in this reaction. Thus, the molecular modeling procedure used here could be applied to predict the regioselectivity of rCE for the acetylation of other cineol derivatives and structurally related compounds.

Experimental

General experimental procedures: Optical rotations were measured on a SEPA-300 HORIBA polarimeter. NMR measurements were recorded on a Bruker 300 AVANCE spectrometer at 300 (^{1}H) and 75 (^{13}C) MHz in $CDCl_3$ solutions containing TMS as internal standard. Melting points were determined on an Ernst Leitz 350 microscope. The rCE samples were purchased from Sigma-Aldrich. Merck silica gel (230-400 mesh, ASTM) was used for column chromatography (CC). Analytical TLC was performed on precoated Merck silica gel 60 F_{254} plates.

Chiral GC-FID analysis: GC-FID analyses were carried out using a Hewlett Packard 5890 Series II gas chromatograph equipped with a flame ionization detector (FID) and a chiral capillary column Cyclosil-B (30 m x 0.25 mm i.d. x 0.25 μm film thickness) (J&W Scientific). Injector and detector temperature were maintained at 250°C and 270°C, respectively. Injection size 0.5 μL, split mode, nitrogen was used as carrier gas at a flow rate of 1.00 mL min^{-1}. The oven was programmed as follows: (a) for acetates (+)-**4** and (-)-**4**: 125ºC (25 min), 125 → 220ºC (10ºC min^{-1}), 220ºC (1 min); Rt (+)-**4**: 15.10 min; Rt (-)-**4**: 14.77 min; (b) (-)-3-acetyloxy-5-hydroxy-1,8-cineole (**6**): 180ºC (3 min), 180 → 240ºC (5ºC min^{-1}), 240ºC (5 min); Rt (-)-**6**: 8.40 min. Percentages (FID) were obtained from electronic integration measurements using an HP 3395 integrator. All the experiments were carried out in triplicate.

GC-MS analysis: Mass spectra were recorded on a 5973 Hewlett Packard selective mass detector coupled to a Hewlett Packard 6890 GC using a HP-5MS (5% phenylmethylsiloxane) capillary column (30 m x 0.25 mm i.d.; 0.25 μm film thickness). The injector, GC-MS interphase, ion source and selective mass detector temperatures were maintained at 250°C, 275°C, 280°C and 150°C, respectively; ionization energy, 70 eV; injection size: 1.0 μL (split mode). Helium was used as carrier gas at a flow rate of 1.0 mL min^{-1}. The oven was programmed as follows: 90°C (2 min), 90 →150ºC (4°C min^{-1}), 150°C (2 min), 150 → 220ºC (6ºC min^{-1}), and then held at 220°C for 5 min.

General procedure for the rCE-catalyzed resolutions: The enzymatic reaction was carried out using rabbit liver esterase (rCE) (EC 232-773-7; Sigma Lot 061K74451) suspension (2,500 units) in buffer 0.1 M Tris, 3.6 M $(NH_4)_2SO_4$ solution, which was added to a solution 70 mM Tris-HCl, 0.3% of Triton X-100 containing the substrate, and then incubated at 37ºC with magnetic stirring. Aliquots (0.2 mL) were taken at different times. Each sample was salted out followed by addition of ethyl acetate (1 mL) twice, and the suspension was vigorously stirred. The organic layer was dried over anhydrous Na_2SO_4, filtered and the solvent evaporated. The residue was monitored by TLC, GC-MS and GC-FID chiral.

(1*R*,3*R*,4*S*)-(-)-3-Hydroxy-1,8-cineole [(-)-**3**] and **(1*S*,3*S*,4*R*)-(+)-3-acetyloxy-1,8-cineole** [(+)-**4**]**:** Enzymatic hydrolysis was carried out following the general procedure described above, using 70 mg (0.33 mmol) of (±)-3-*endo*-acetyloxy-1,8-cineole [(±)-**4**] at pH 8.5. In parallel we performed a test without rCe in order to estimate the unspecific hydrolysis rate. Our results indicated that this rate is about 8%. After incubation for 13 d the mixture was salted out, extracted with ethyl acetate (3 x 20 mL), the organic extract was dried over anhydrous Na_2SO_4, filtered, the solvent was removed under reduced pressure and the residue containing the ester/alcohol mixture was chromatographed on Si gel with *n*-hexane-EtOAc mixtures as eluent to yield (1*S*,3*S*,4*R*)-(+)-3-acetyloxy-1,8-cineole [(+)-**4**] (33.6 mg, 48%), $[\alpha]_D$= +47.83 (*c* 2.86, $CHCl_3$), 90.8% ee and (1*R*,3*R*,4*S*)-(-)-3-hydroxy-1,8-cineole [(-)-**3**] (31.5 mg, 45%), $[\alpha]_D$= -54.47 (*c* 4.00, $CHCl_3$), as crystalline solids. The compounds

showed MS, ^{1}H- and ^{13}C-NMR data identical to those previously reported [1].

(1*S*,3*S*,4*R*,5*R*)-(-)-3-Acetyloxy-5-hydroxy-1,8-cineole (**6**): Diacetate **5** was asymmetrized with rCE following the general procedure described above at pH 8.5. From 30 mg (0.11 mmol) of **5** and after incubation for 4 d (28 mg, 90%) (1S,3S,4R,5R)-(-)-3-acetyloxy-5-hydroxy-1,8-cineole (**6**) was isolated as a colorless oil, $[\alpha]_D$ = -1.57 (*c* 4.7, $CHCl_3$). GC quiral analysis showed that the remaining monoacetate was enantiomerically pure. The MS, ^{1}H- and ^{13}C-NMR data were identical to those reported [1].

Molecular modeling

Tertiary structure prediction of rCE validation: The first step in this study was to choose the optimal rCE structure to be used in the docking analyses. In our simulations we used the rCE structure reported by Bencharit *et al.* [2]. Such a structure was determined by molecular replacement using the structure of *Torpedo californica* acetylcholinesterase (tAcChE) as a search model [25] and refined to 2.5 Å of resolution. It is interesting to note that in the structure reported by Bencharit *et al.* [2], residues 355-370 (loop 1) and 450-466 (loop 2) are not reported in the final model (Figure 2). The rCE 3-D homology models were built based on the 3-D structure of rCE (PDB codes: 1K4Y [2], 1THG and 2BCE) using the Swiss-Model server [26,27]. The 3-D models were subsequently analyzed and selected according to the best fit of the sequence identity. The best identity (94%) was the rCE model with PDB code: 1K4Y, which was used for subsequent steps. This alignment was the input for MD. Then, the protonation state (pH= 7) of the residues of the rCE model was edited by the program pdb2gmx, which is included in the GROMACS program [28].

Choice of the optimal rCE structure for docking: In order to complete the sequence of rCE, the NCBI protein data base [http://www.ncbi.nlm.nih.gov/sites/entrez] was used to search the sequence of amino acids for rCE. The complete sequence was reported by Potter (AAC39258, entry name AF036930.1, 565 amino acids) [29].

Automated docking setup: All the docking calculations were performed by using AutoDock 4.0 [30]. rCE esterase was first modified by adding polar hydrogens and then kept rigid in docking processes. All the torsional bonds of ligands were set free by the Ligand module in AutoDock Tools package of programs. The docking area was defined by a box, centered on the Cα of the Ser221 residue. Grid points of 60 x 60 x 60 with 0.375 Å spacing were calculated around the docking area for all the ligand atom types using AutoGrid. Gasteiger charges were assigned and non-polar hydrogen atoms were merged. All torsions were allowed to rotate during docking. The docking energy grid was produced with the auxiliary program AutoGrid. The center of the ligand was positioned at the grid center. All graphic manipulations and visualizations were performed by means of the AutoDock Tools [31] and Chimera [32] programs. The Lamarckian genetic algorithm was utilized and the energy evaluations were set at 2.5×10^{6}. A total of 250 accepted conformations were collected. Other parameters were set to default values. The docking results from each of the 50 calculations were clustered on the basis of root-mean square deviation (rmsd) between the Cartesian coordinates of the ligand atoms and were ranked according to the binding free energy. The structure with relative lower binding free energy and the most cluster members was chosen for the optimum docking conformation.

MD simulations: A 3D model of the rCE was used for the Molecular Dynamics (MD) simulations, based on the X-ray structure of Bencharit *et al.* [2] (PDB acquisition code: 1K4Y). The ligands topologies were built using partial charges obtained from fitting to electrostatic potential surfaces (EPS) with the CHELPG procedure [33,34]. In the present study, we have used an approach where automatic docking was guided by using AutoDock 4.0 [30]. Thus, these receptor–ligand complexes were prepared in order to obtain the input files for MD runs. Several docking positions were considered and the strongest receptor interactions were examined in detail.

The MD simulations and analysis were performed using the GROMACS 4.0 simulation package [33,34] with the OPLS-AA force field [34 28, 35-38] and the SPC water model [39,40] in a cubic box with periodic boundary conditions. The receptor-ligand complexes were embedded in a box containing the SPC water model that extended to at least 1 nm between the receptor and the edge of the box resulting in a box of 9.2 nm of side lengths. The total number of water molecules was 19362 for the different simulations. Then four Na^{+} ions were added to the systems by replacing water in random positions, thus making the whole system neutral. The time step for the simulations was 0.002 ps for a complete simulation time of 2 ns. For long-ranged interactions, the article-mesh Ewald (PME) [41 40-42] method was used with a 1 nm cut-off and a Fourier spacing of 0.12 nm. The MD protocol consisted of several preparatory steps; energy minimization using the conjugate gradient model [43,44], density stabilization (NPT conditions), and finally production of the MD simulation trajectory. All production simulations were performed under NVT conditions at 298 K, using v-rescale coupling algorithm [44] for keeping the temperature constant. The compressibility was 4.8×10^{-5} bar^{-1}. All coordinates were saved every 5 ps. The SETTLE [40 38] algorithm was used to keep water molecules rigid. The analysis of the simulations was performed using the analysis tools provided in the Gromacs package [28 34].

Acknowledgements - The authors thank Consejo de Investigaciones de la Universidad Nacional de Tucumán (CIUNT, projects 26/D416 and 26/D458) and Consejo Nacional de Investigaciones Científicas y Técnicas de Argentina (CONICET). This research was partially supported by grants from Universidad Nacional de San Luis and CONICET. RDE is a member of the CONICET (Argentina) staff.

References

[1] Loandos MH, Villecco MB, Burgueño-Tapia E, Joseph-Nathan P, Catalán CAN. (**2009**) Preparation and absolute configuration of (1*R*,4*R*)-(+)-3-oxo-, (1*S*,4*S*)-(-)-3-oxo- and (1*R*,3*S*,4*R*)-(+)-3-acetyloxy-5-oxo-1,8-cineole. *Natural Product Communications*, ***4***, 1537-1545.

[2] Bencharit S, Morton CL, Howard-Williams EL, Danks MK, Potter PM, Redinbo MR. (**2002**) Structural insights into CPT-11 activation by mammalian carboxylesterases. *Nature Structural & Molecular Biology*, ***9***, 337-342.

[3] Williams FM. (**1985**) Clinical significance of esterases in man. *Clinical Pharmacokinetics*, ***10***, 392-403.

[4] Joly JM, Brown TM. (**1986**) Metabolism of aspirin and procaine in mice pretreated with o-4-nitrophenyl methyl(phenyl)phosphinate or o-4-nitrophenyl diphenylphosphinate. *Toxicology and Applied Pharmacology*, ***84***, 523-532.

[5] Brzezinski MR, Spink BJ, Dean RA, Berkman CE, Cashman JR, Bosron WF. (**1997**) Human liver carboxylesterase hCE-1: Binding specificity for cocaine, heroin, and their metabolites and analogs. *Drug Metabolism and Dispositions*, ***25***, 1089-1096.

[6] Kamendulis LM, Brzezinski MR, Pindel EV, Bosron WF, Dean RAJ. (**1996**) Metabolism of cocaine and heroin is catalyzed by the same human liver carboxylesterases. *Journal of Pharmacology and Experimental Therapeutics*, ***279***, 713-717.

[7] Lotti M, Ketterman A, Waskell L, Talcott RE. (**1983**) Meperidine carboxyesterase in mouse and human livers. *Biochemical Pharmacology*, ***32***, 3735-3738.

[8] Morton CL, Potter PM. (**2000**) Comparison of *Escherichia coli*, *Saccharomyces cerevisiae*, *Pichia pastoris*, *Spodoptera frugiperda*, and COS7 cells for recombinant gene expression: Application to a rabbit liver carboxylesterase. *Molecular Biotechnology*, ***16***, 193-202.

[9] Otwinowski Z, Minor W. (**1993**) In *Data Collection and Processing*. Sawyer L, Isaacs N, Bailey S. (Eds). SERC Daresbury Laboratory, Warrington, UK, 556–562.

[10] Matthews BW. (**1968**) Solvent content of protein crystals. *Journal of Molecular Biology*, ***33***, 491-497.

[11] Navaza J, Saludjian P. (**1997**) AMoRe: An automated molecular replacement program package. *Methods in Enzymology*, ***276***, 581-594.

[12] Ollis DL, Cheah E, Cygler M, Dijkstra B, Frolow F, Franken M, Harel SJ, Remington I, Silman J, Schrag JL, Sussman KHG, Verschueren A, (**1992**) The α/β hydrolase fold. *Protein Engineering*, ***5***, 197-211.

[13] Brünger AT, Adams PD, Clore GM, DeLano WL, Gros P, Grosse-Kunstleve RW, Jiang JS, Kuszewski J, Nilges M, Pannu NS, Read RJ, Rice LM, Simonson T, Warren GL. (**1998**) Crystallography & NMR system: A new software suite for macromolecular structure determination. *Acta Crystallographica Section D: Biological Crystallography*, ***54***, 905-921.

[14] Danks MK, Morton CL, Krull EJ, Cheshire PJ, Richmond LB, Naeve CW, Pawlik CA, Houghton PJ, Potter PM. (**1999**) Comparison of activation of CPT-11 by rabbit and human carboxylesterases for use in enzyme/prodrug therapy. *Clinical Cancer Research*, ***5***, 917-924.

[15] Read RJ. (**1986**) Improved Fourier coefficients for maps using phases from partial structures with errors. *Acta Crystallographica Section A*, ***42***, 140-149.

[16] Bosron WF, Hurley TD. (**2002**) Lessons from a bacterial cocaine esterase. *Nature Structural & Molecular Biology*, ***9***, 4-5.

[17] Laskowski RA, McArthur MW, Moss DS, Thornton JMJ. (**1993**) PROCHECK: a program to check the stereochemical quality of protein structures. *Applied Crystallography*, ***26***, 283-291.

[18] Kazlauskas RJ. (**2000**) Molecular modeling and biocatalysis: Explanations, predictions, limitations, and opportunities. *Current Opinion in Chemical Biology*, ***4***, 81-88.

[19] Braiuca P, Ebert C, Basso A, Linda P, Gardossi L. (**2006**) Computational methods to rationalize experimental strategies in biocatalysis. *Trends in Biotechnology*, ***24***, 419-425.

[20] Vain Lith HA, Haller M, van Zutphen BFM, Beynen AC. (**1992**) Substrate specificity of purified rabbit liver esterase ES-1. *European Journal of Biochemistry*, ***206***, 527-535.

[21] James JJ, Lakshmi BS, Raviprasad V, Ananth MJ, Kangueane P, Gautam P. (**2003**) Insights from molecular dynamics simulations into pH-dependent enantioselective hydrolysis of ibuprofen esters by *Candida rugosa* lipase. *Protein Engineering*, ***16***, 1017-1024.

[22] Loandos MH, Muro AC, Villecco MB, Catalán CA. (**2006**) Stereospecificity of pig liver esterase in the hydrolysis of racemic esters derived from 1,8-cineole. *Molecular Medicinal Chemistry*, ***10***, 35-37.

[23] Davis AM, Teague SJ. (**1999**) Hydrogen bonding, hydrophobic interactions, and failure of the rigid receptor hypothesis. *Angewandte Chemie International Edition*, ***38***, 736-749.

[24] Luzzio FA, Duveau DY. (**2002**) Enzymatic resolution of the 1,3,3-trimethyl-2-oxabicyclo[2.2.2]octane (1,8-cineole) system. *Tetrahedron-Asymmetry*, ***13***, 1173-1180.

[25] Harel M, Schalk I, Ehret-Sabatier L, Bouet F, Goeldner M, Hirth C, Axelsen PH, Silman I, Sussman JL. (**1993**) Quaternary ligand binding to aromatic residues in the active-site gorge of acetylcholinesterase. *Proceeding of National Academy of Sciences of the United States of America*, ***90***, 9031-9035.

[26] Schwede T, Kopp J, Guex N, Peitsch MC. (**2003**) SWISS-MODEL: An automated protein homology-modeling server. *Nucleic Acids Research*, ***31***, 3381-3385.

[27] Guex N, Peitsch MC. (**1997**) SWISS-MODEL and the Swiss-PdbViewer: An environment for comparative protein modeling. *Electrophoresis*, ***18***, 2714-2723.

[28] Hess B, Kutzner C, van der Spoel D, Lindahl E. (**2008**) GRGMACS 4: Algorithms for highly efficient, load-balanced, and scalable molecular simulation. *Journal of Chemical Theory and Computation*, ***4***, 435-447.

[29] Potter PM, Pawlik CA, Morton CL, Naeve CW, Danks MK. (**1998**) Isolation and partial characterization of a cDNA encoding a rabbit liver carboxylesterase that activates the prodrug irinotecan (CPT-11). *Journal of Cancer Research*, ***58***, 2646-2651.

[30] Morris GM, Goodsell DS, Halliday RS, Huey R, Hart WE, Belew RK, Olson AJ. (**1998**) Automated docking using a Lamarckian genetic algorithm and an empirical binding free energy function. *Journal of Computational Chemistry*, ***19***, 1639-1662.

[31] Sanner MF. (**1999**) Python: A programming language for software integration and development. *Journal of Molecular Graphics and Modelling*. ***17***, 57-61.

[32] Pettersen EF, Goddard TD, Huang CC, Couch GS, Greenblatt DM, Meng EC, Ferrin TE. (**2004**) UCSF Chimera - A visualization system for exploratory research and analysis. *Journal of Computational Chemistry*. ***25***, 1605-1612.

[33] Berendsen HJC, van der Spoel D, van Drunen R. (**1995**) GROMACS: A message-passing parallel molecular dynamics implementation. *Computer Physics Communications*, ***91***, 43-56.

[34] Lindahl E, Hess B, van der Spoel D. (**2001**) GROMACS 3.0: A package for molecular simulation and trajectory analysis. *Journal of Molecular Modelling*, ***7***, 306-317.

[35] Jorgensen WL, Maxwell DS, Tirado-Rives J. (**1996**) Development and testing of the OPLS all-atom force field on conformational energetics and properties of organic liquids. *Journal of American Chemical Society*, ***118***, 11225-11236.

[36] Jorgensen WL, McDonald NA. (**1998**) Development of an all-atom force field for heterocycles. Properties of liquid pyridine and diazenes. *Journal of Molecular Structure*, ***424***, 145-155.

[37] Rizzo RC, Jorgensen WL. (**1999**) OPLS all-atom model for amines: Resolution of the amine hydration problem. *Journal of American Chemical Society*, ***121***, 4827-4836.

[38] Miyamoto S, Kollman PA. (**1992**) SETTLE: An analytical version of the SHAKE and RATTLE algorithm for rigid water models. *Journal of Computational Chemistry*, ***13***, 952-962.

[39] Berendsen HJC, Postma JPM, van Gunsteren WF, Hermans WF. (**1983**) Interaction models for water in relation to protein hydration. In *Intermolecular forces*. B. Pullman ed., Reidel, Dordrecht. 331-342.

[40] Darden T, York D, Pedersen L. (**1993**) Particle mesh Ewald: An N-log(N) method for Ewald sums in large systems. *Journal of Chemical Physics*, ***98***, 10089-10092.

[41] Essmann U, Perera L, Berkowitz ML, Darden T, Lee H, Pedersen LG. (**1995**) A smooth particle mesh Ewald method. *Journal of Chemical Physics.* ***103***, 8577-8593.

[42] Luty B, Tironi IG, van Gunsteren WF. (**1995**) Lattice-sum methods for calculating electrostatic interactions in molecular simulations. *Journal of Chemical Physics*, ***103***, 3014-3021.
[43] Fergusson DM. (**1995**) Parameterization and evaluation of a flexible water model. *Journal of Computational Chemistry*, ***16***, 501-511.
[44] Berendsen HJC, Postma JPM, DiNola A, Haak JR. (**1984**) Molecular-dynamics with coupling to an external bath. *Journal of Chemical Physics*, ***81***, 3684-3690.